ANALYSIS OF THE MATERIAL REMOVAL IN HYBRID ELECTROCHEMICAL-ULTRASONIC MACHINING OF A 12% Cr STAINLESS STEEL

Cornel-Cristian Enciu[1], Liviu-Daniel Ghiculescu[2]
[1] National University of Science and Technology, "Politehnica", Bucharest, *Corresponding author*, ORCID No. 0000-0001-8905-4571, cornel.enciu@upb.ro
[2] National University of Science and Technology, "Politehnica", Bucharest, ORCID No. 0000-0001-6963-8350, daniel.ghiculescu@upb.ro

ABSTRACT: The paper deals with the presentation of an analysis for material removal process in the hybrid electrochemical-ultrasonic machining of a 12% Cr stainless steel. The Comsol Multiphysics software was used for the numerical simulation of the material removal process of the 12% Cr stainless steel. It was necessary to parameterize the models in order to study the behavior of the steel with Cr carbide constituents. A scanning electron microscope from POLITEHNICA University of Bucharest, named SEM QUANTA INSPECT F50, was employed to highlight the morphological structure of the machined surfaces. The influence of the material removal process on surface roughness was studied by varying the parameters of consumed ultrasonic power and current intensity.
KEYWORDS: electrochemical machining, simulation, roughness, modeling.

1. INTRODUCTION

Electrochemical machining (ECM) is well-known as a nonconventional manufacturing technology used in various industries (automotive, aerospace, medical, electronics, etc.) to produce surfaces that generally cannot be obtained by applying classical machining technologies [1, 2]. The main advantages of ECM compared to conventional technologies are the material removal rate does not depend on its hardness, and there is no tool wear during machining [3, 4].
The principle for the material removal is based on anodic dissolution, according to Faraday's laws of electrolysis [5], with the electrochemical dissolution process taking place in an electrolytic solution [2, 6].
To increase productivity and the quality of the resulting surface, ultrasonic machining can be combined with electrochemical machining, thus forming a hybrid technology, electrochemical-ultrasonic machining (ECM+US). Vibrations can be applied to the tool, the workpiece, or the electrolytic solution. In addition to the advantages of electrochemical machining, like material removal rate (MRR) and zero tool wear, one benefit of adding ultrasonic vibrations is the elimination of the passivated layer formed on the machined surface, leading to improved roughness. The application of ultrasound in hybrid electrochemical machining promotes the removal of the passivated layer through ultrasonic cavitation.
As a working method, vibrations can be applied simultaneously with electrochemical machining or successively, while varying the current density, the machining gap or the machining time.

The study presented in this paper focuses on hybrid electrochemical-ultrasonic machining of a 12% Cr stainless steel, using a 5% sodium chloride solution (5% NaCl) as the electrolytic liquid.

2. NUMERICAL SIMULATION OF THE REMOVAL PROCESS OF A 12% Cr STAINLESS STEEL

In order to study the influence of Cr carbide particle components, new models were developed using the finite element method with the specialized software, Comsol Multiphysics. These models formed the basis for the numerical simulation of the ultrasonic component of the hybrid electrochemical-ultrasonic machining process. The introduction of Cr carbide particles into the material structure is also compatible with the study of the behavior of 12% Cr stainless steel, which was used to produce the test parts.
The Structural Mechanics, Time Dependent module was used, taking into account the very short duration of the load corresponding to the collective implosion of gas bubbles at the end of the extension half-cycle of the electrolytic liquid, associated with ultrasonic-induced cavitation in the machining gap.
The first step was to introduce the parameters of the models as can be seen in figure 1.
Then, a parameterized geometry of the models (Figure 2) was created using the drawing tools in Comsol Multiphysics, placing Cr carbide particles of

submicron size in various positions of interest-closer (a) or farther (b) from the area of the micropeaks of the machined surface microgeometry.

Parameters

Name	Expression	Value	Description
hp	5[mm]	0.005 m	workpiece height
lp	20[mm]	0.02 m	workpiece width
Ra	1.6e-6	1.6E-6	surface roughness before ECM
PRa	0.1[mm]	1.0E-4 m	micro-irregularity pitch
acr	PRa/2	5.0E-5 m	radius of micro-depressions before ECM
bcr	4*Ra	6.4E-6	depth of micro-depressions before ECM
pf	0.5e-6	5.0E-7	passivation film thickness at microgeometry peaks
tus	6e-5	6.0E-5	cavitation bubble collapse time
pus	150[MPa]	1.5E8 Pa	ultrasonic cavitation pressure
modulFe2O3	300[GPa]	3.0E11 Pa	Young's modulus of iron oxide
roFe2O3	4345	4345	iron oxide density
nuPFe2O3	0.24	0.24	Poisson's ratio of iron oxide
tau0Fe2O2	55.55	55.55	shear fatigue strength [MPa] of iron oxide
acrCrC	0.2e-6	2.0E-7	large radius of Cr carbide particle
bcrCrC	0.05e-6	5.0E-8	small radius of Cr carbide particle

Figure 1. Parameterization of the models for studying the behavior of steels with Cr carbide constituents

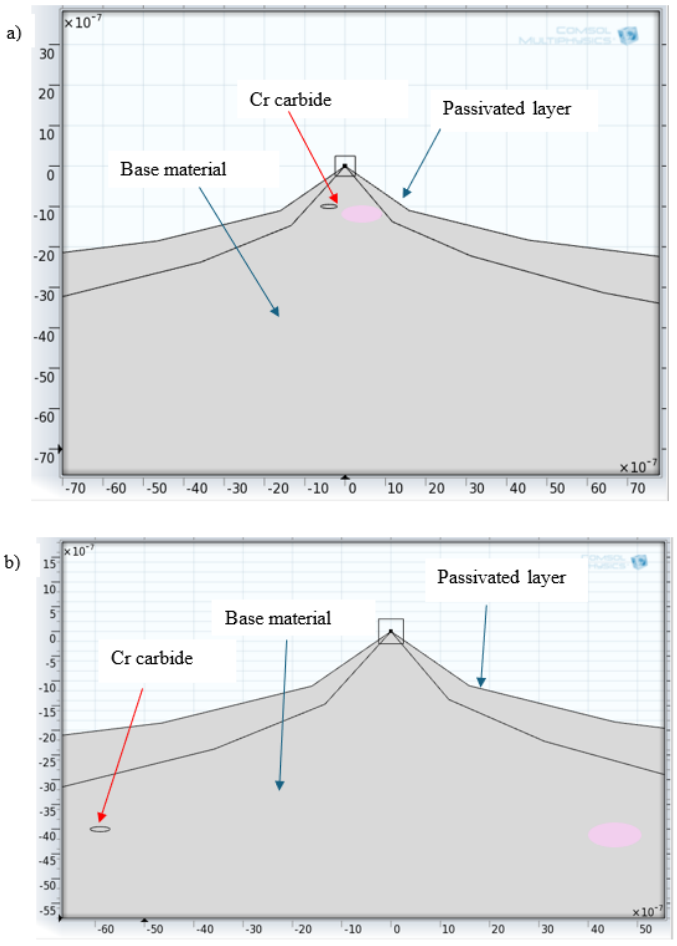

Figure 2. Creation of the model geometry with Cr carbide particles

The assignment of material properties for Cr carbides is shown in figure 3.

Materials	Property	Name	Value	Unit
D3 (UNS T30403) [solid]	Density	rho	6600[kg/m^3]	kg/m^3
Iron Oxide	Young's modulus	E	380[GPa]	Pa
Cr Carbide	Poisson's ratio	nu	0.3	1

Materials	Property	Na...	Value	Unit
D3 (UNS T30403) [solid]	Density	rho	15700[kg/m^3]	kg/m^3
Iron Oxide	Young's modulus	E	680[GPa]	Pa
Cr Carbide	Poisson's ratio	nu	0.3	1

Figure 3. Assignment of material properties for Cr carbide particles

The allowable stress values for Cr carbide, was determined using equation (1) and information regarding static loads [7, 8].

$$\tau_0 = 1{,}2(40+0{,}16\cdot\sigma_r)\ [\text{MPa}] \qquad (1)$$

where the parameter σ_r is the static tensile strength.

For Cr carbide, τ_0 = 247,488 MPa

The areas where material is removed were visualized, where the unit stresses exceed the τ_0 parameters determined for 12% Cr stainless steel in case (a), with particles placed closer to the micropeak zone (Figure 4), and in case (b), farther from the micropeak zone (Figure 5).

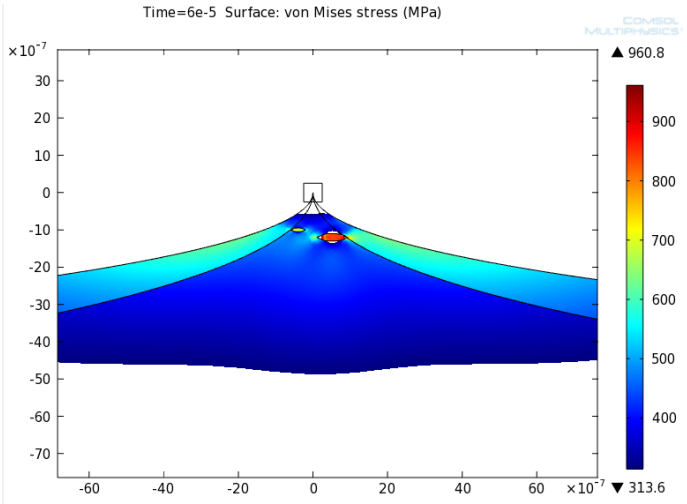

Figure 4. Von Mises unit stresses for carbide particles positioned relatively close to the micropeak zone

It can be observed that in this case, figure 4, the maximum unit stress exceeds the fatigue strength; therefore, the particles can be removed at an ultrasonic pressure of pus=150MPa in this case.

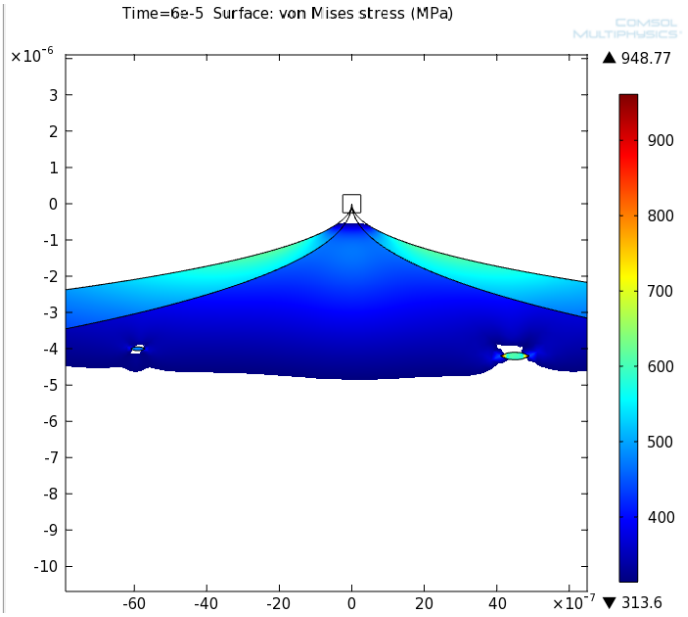

Figure 5. Von Mises unit stresses for carbide particles at the material removal threshold position

As a result of the chromium carbides, the material removal caused by ultrasonically induced cavitation in the machining working gap is non-uniform, which creates difficulties in the process of improving the surface roughness of the machined part.

3. ELECTRON SCANNING ANALYSIS OF THE REMOVAL PROCESS OF 12% Cr STAINLESS STEEL

To analyse the morphological structure of the machined surfaces depending on the processing parameters used, a scanning electron microscope, named SEM QUANTA INSPECT F50, from POLITEHNICA University of Bucharest was employed, as illustrated in figure 6. It includes Schottky field-emission electron source, with high resolution of up to 1.2 nm, and Energy Dispersive X-ray spectroscopy (EDS) analysis to determine elemental composition.

It can be seen the clamping device where the workpiece has to be positioned for the analysis of the morphological structure. The analysis is realised in the whole area of the machined surface and a very important objective is to observe the uniformity of the technology applied.

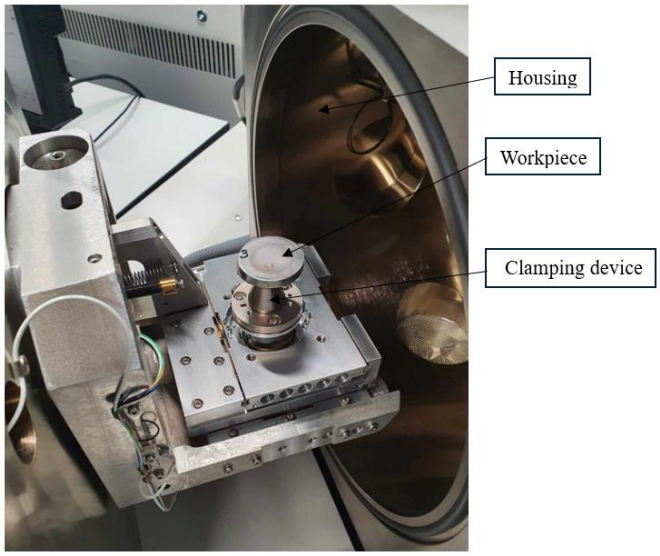

Figure 6. SEM QUANTA INSPECT F50 - Part positioning

Some of the results provided by SEM for the test parts finished by electrochemical machining are presented, allowing a comparison with the results obtained from the hybrid electrochemical-ultrasonic machining process.

With the increase in current density (Figure 7), by raising I, the thickness of the material layer was greater, and consequently, Cr carbide particles can also be observed, generally around 100 nm in size and, more rarely, exceeding 1 μm. It is possible to remove the material adjacent to a Cr carbide particle, and implicitly the carbide itself, resulting in cavities on the micrometer scale.

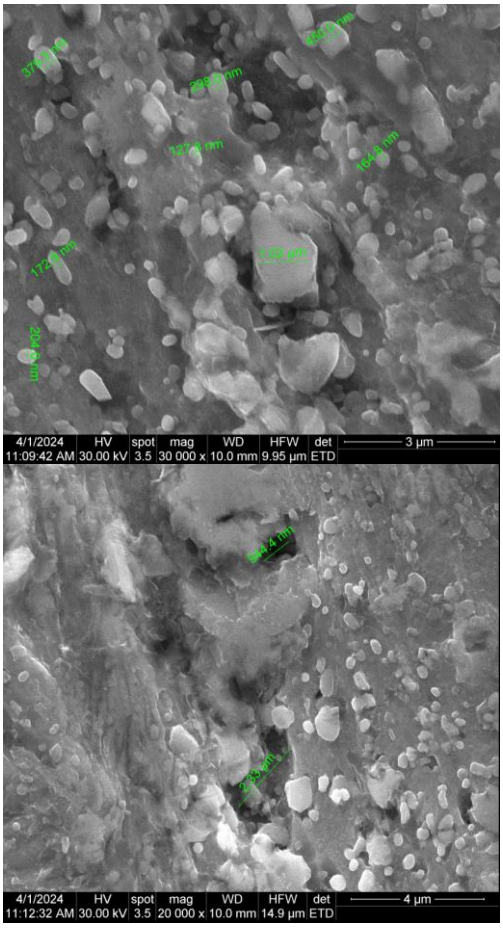

Figure 7. SEM images of the surfaces of a 12% Cr stainless steel sample, processed by ECM with I = 0.75 A, s_F = 0.6 mm, t = 3 min, Ra decrease 19.27%

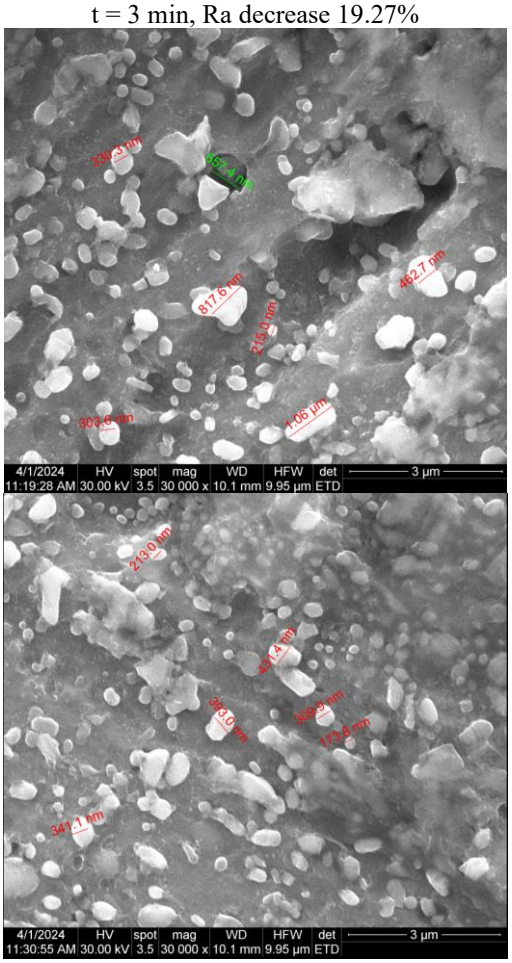

Figure 8. SEM images of the surfaces of a 12% Cr stainless steel sample, processed by ECM with I = 1 A, s_F = 0.6 mm, t = 3 min, Ra decrease of 23.1%

With a further increase in current density, J=0.204 A/cm^2 for a current of I=1A (Figure 8), a maximum improvement for the roughness parameter, Ra, of the machined part is observed, with a reduction of 23.1%, which can be explained by the removal of microgeometry peaks.

The data provided by SEM for a series of 12% Cr stainless steel test parts, finished by successive electrochemical-ultrasonic machining, are presented, maintaining the current density while increasing the power applied to the ultrasonic system.

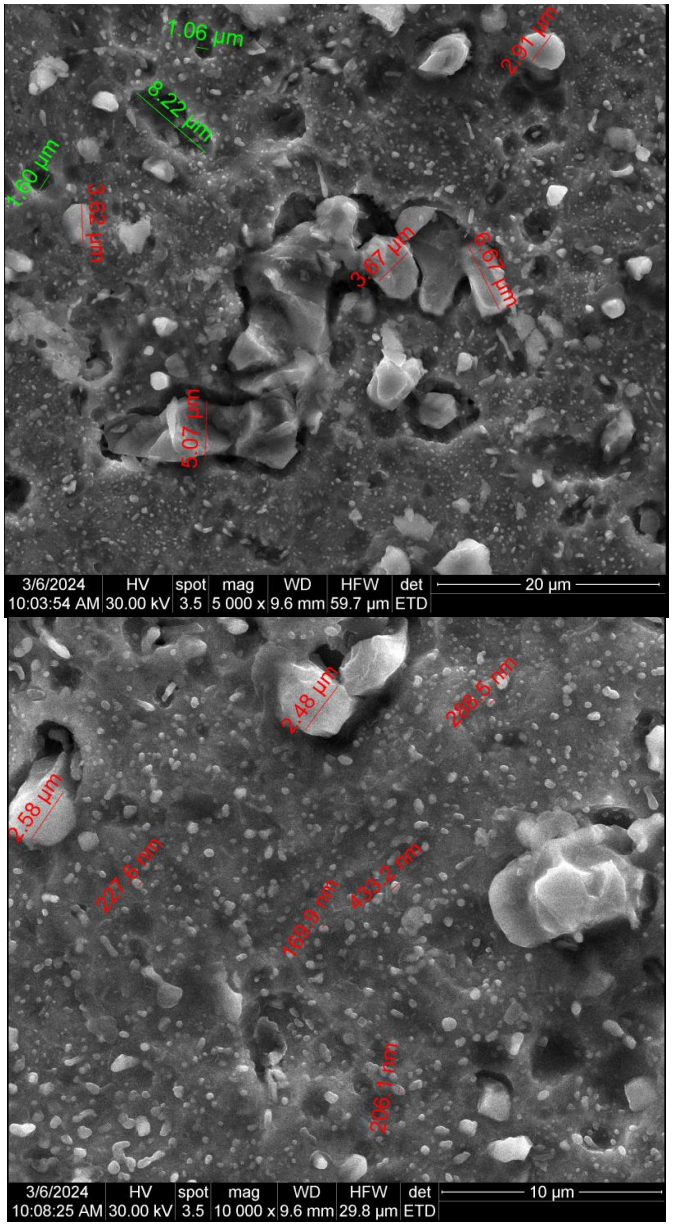

Figure 9. SEM images of the surfaces of a 12% Cr stainless steel sample, processed by successive ECM + US with P = 109.2 W, I = 1.5 A, s_F = 0.7 mm, Ra decrease of 25.58%

In figure 9, an improvement in the surface roughness of the machined part can be observed as a result of additional smoothing achieved by increasing the power applied to the ultrasonic system, which ensures further removal of micropeaks, as previously demonstrated in the modeling and numerical simulation of the ECM+US finishing process.

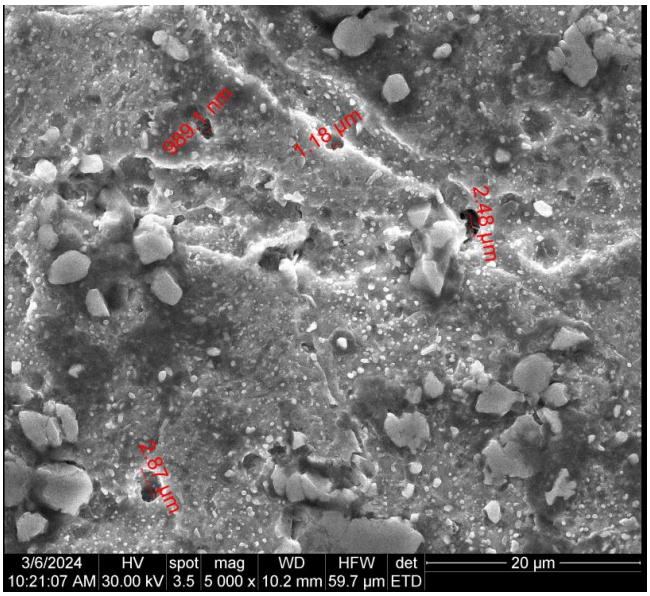

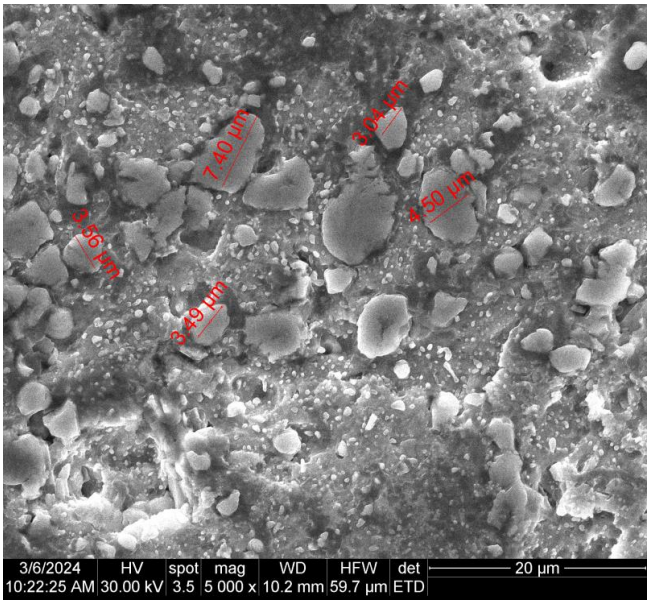

Figure 10. SEM images of the surfaces of a 12% Cr stainless steel sample, processed by successive ECM + US with P = 114 W, I = 1.5 A, s_F = 0.7 mm, Ra decrease of 29.06%

A further increase in the power applied to the ultrasonic system ensures an improvement in the surface roughness of the machined part (Figure 10), corresponding to additional material removal from the micropeak zones.

When the power applied to the ultrasonic system is increased to the maximum value used in these experiments (Figure 11), material is also removed from the microdepression areas, which tends to reduce the improvement in the surface roughness of the machined part.

The optimal value has been exceeded, as previously demonstrated in the modeling and numerical simulation of the ECM+US finishing process.

Thus, current density, variation of the working gap value, as well as processing time are extremely important factors in the machining of different materials, not only of 12% Cr stainless steel.

For each material, certain specific optimal values can be identified, depending on its characteristics, so that the main parameter of interest, surface roughness, has the lowest possible values.

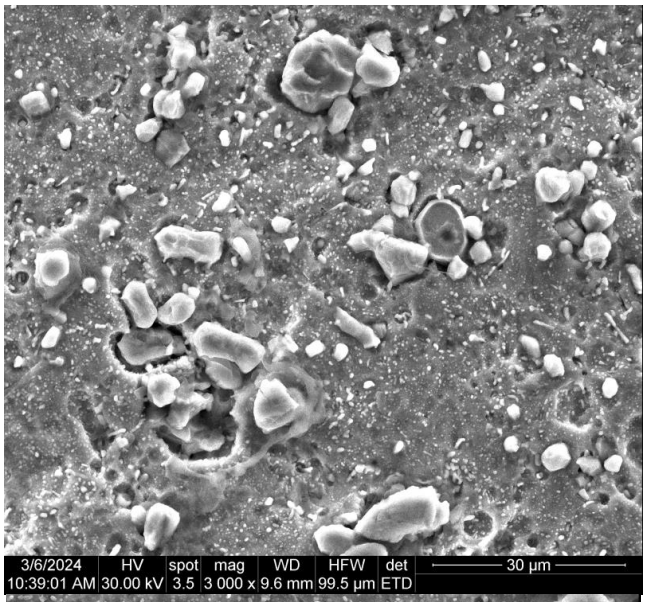

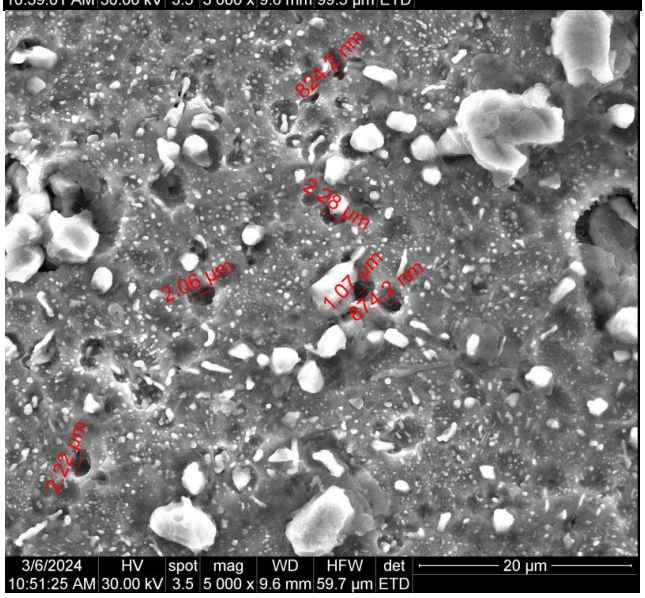

Figure 11. SEM images of the surfaces of a 12% Cr stainless steel sample, processed by successive ECM + US with P = 118.8 W, I = 1.5 A, s_F = 0.7 mm, Ra decrease of 25.1%

The study realised using the SEM QUANTA INSPECT F50 scanning electron microscope shows that the parts are made of a medium-quality stainless steel belonging to the ferritic class.

The bright, cuboidal particles represent chromium carbides (likely with the chemical formulas $Cr_{23}C_6$ or Cr_7C_2).

Other particles with similar brightness and regular polyhedral morphology, but smaller in size, may also be chromium carbides. Both the large, bright white particles and the smaller ones exhibit a high density, suggesting reduced corrosion resistance, particularly to intergranular corrosion, which drastically lowers the mechanical strength characteristics.

This material structure may result from prolonged thermal or radiation exposure, which favored the formation of Cr carbides. The smallest particles, on the nanometer scale, with somewhat more rounded shapes compared to the others and distributed as a fine bright dispersion, may be oxides or other oxygenated corrosion products.

The EDAX (energy-dispersive X-ray detector) analysis was performed. The advantage of the method lies in the fact that it allows a rapid, non-destructive, and localized analysis, even on very small areas of the material.

Figure 12 shows the graphical representation of the percentage composition of the elements in the base material for the 12% Cr stainless steel test samples.

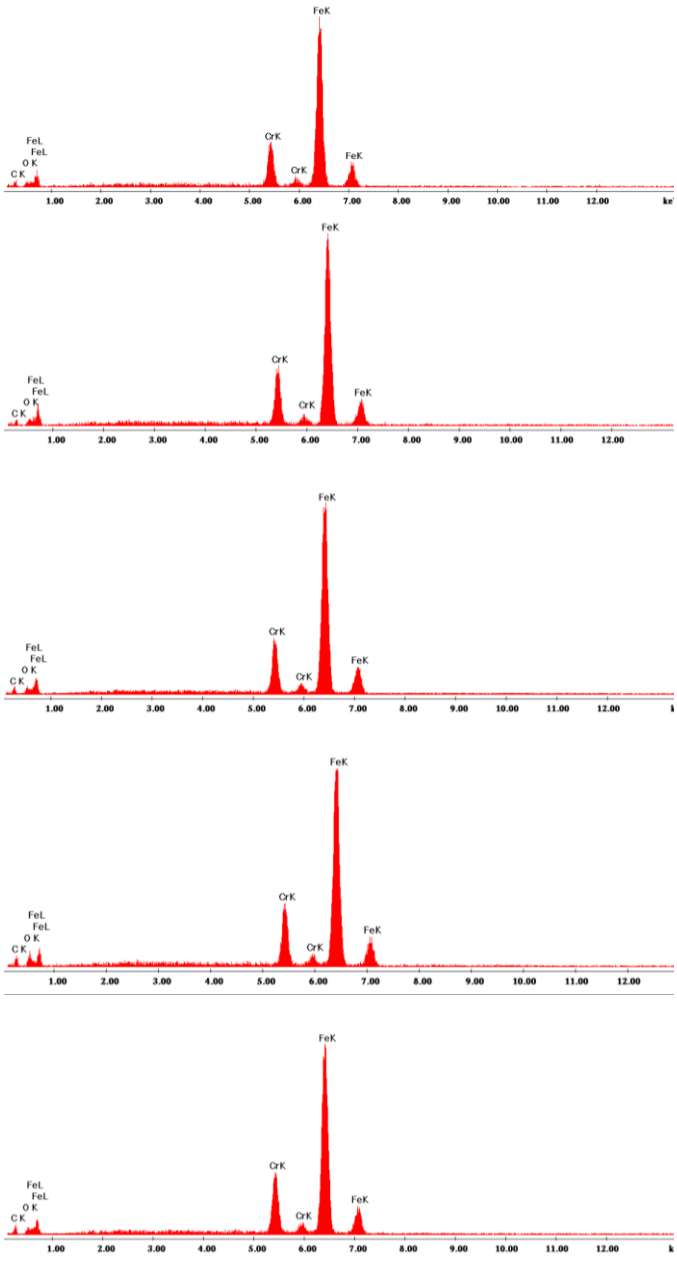

Figure 12. Graphical representation of the percentage composition of the elements in the base material for the 12% Cr stainless steel test samples provided by EDAX

4. THE INFLUENCE OF THE WORKING PARAMETERS ON ROUGHNESS

- The influence of current density on the surface roughness in electrochemical finishing

The testing method involved machining stainless steel test parts (12% Cr, 0.3% C) by simple electrochemical finishing for comparison with hybrid machining processes, with the machining parameters and surface roughness results presented in table 1.

Table 1. ECM machining, s_F = 0.5 mm, stainless steel 12% Cr

Number of testing part	J [A/cm²]	I [A]	Time [min]	Initial Ra [µm]	Ra ECM [µm]	Decrease of Ra [%]
1	0.3	1.47	1 min 30 s	0.606	0.583	3.795
2	0.35	1.71	1 min 30 s	0.896	0.843	5.915
3	0.4	1.96	1 min 30 s	0.874	0.783	10.412
4	0.45	2.2	1 min 30 s	0.52	0.45	13.462
5	0.5	2.45	1 min 30 s	0.779	0.647	16.945

The current density on the machined surface was varied, considering that in this type of processing J must not exceed 0.5 A/cm², and taking into account both the dimensions of the processed test parts and the size of the tool used for ECM finishing.

The electrolyte flow of 5% NaCl was maintained for approximately 1 minute, followed by a 30 second pause to stabilize the electrolyte and to ensure a uniform kinetic distribution so as to avoid significant variations in current intensity.

Electrochemical machining was then carried out for 1 minute and 30 seconds. To remove the passivated layer, a washing step was performed in the frontal gap between the tool and the test parts for 30 seconds.

Surface roughness Ra was measured in three points of each test part using a device specific for measuring this parameter (INSIZE ISR-C002), with the process repeated after the parts were finished by electrochemical machining, and the mean Ra value across the three points was then determined.

The frontal working gap set for ECM processing was 0.5 mm. Under these conditions, an improvement in the surface roughness of up to 16.9% was observed with increasing current density J.

Figure 13 shows the reduction in Ra roughness (the difference between Ra before and after machining) as a function of current density for the electrochemical machining of 12% Cr stainless steel test parts.

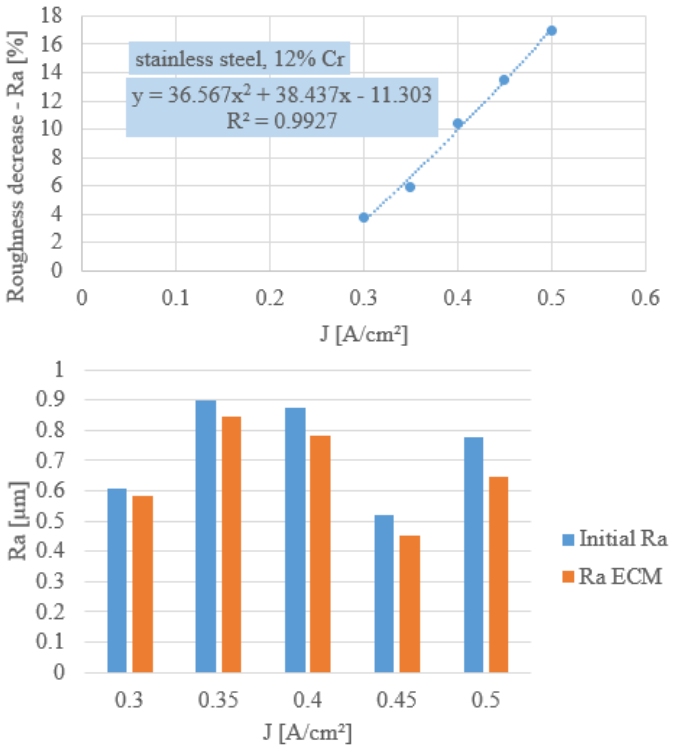

Figure 13. Influence of current density, J, on Ra, s_F = 0.5 mm, 5% NaCl solution, 12% Cr stainless steel

The Ra values show that, when applying this method to 12% Cr stainless steel, an improvement in the surface roughness obtained by ECM finishing is achieved as the current density J increases. However, in addition to the parameter J, other input parameters of the machining process, such as flow rate and solution concentration in the machining gap, also play a role. These parameters must be controlled in order to achieve a significant improvement in Ra.

Then, the current density was varied at a frontal gap value of s_F = 0.6 mm as can be seen in table 2.

For the electrochemical machining of the test parts whose results are presented in table 2, the electrolyte flow of 5% NaCl was maintained for approximately 1 minute, followed by a 30 second pause to stabilize the electrolyte in order to avoid major variations upon the application of current intensity. The electrochemical machining was then carried out for 3 minutes, and the process was completed with a 30 second washing step in the machining gap to remove the passivated layer.

Table 2. ECM machining, s_F = 0.6 mm, 12% Cr stainless steel

Number of testing part	J [A/cm²]	I [A]	Time [min]	Initial Ra [µm]	Ra ECM [µm]	Decrease of Ra [%]
1	0.102	0.5	3	0.298	0.258	13.42
2	0.153	0.75	3	0.41	0.331	19.27
3	0.204	1	3	0.29	0.223	23.10
4	0.306	1.5	3	0.4	0.318	20.50
5	0.408	2	3	0.44	0.393	10.68

Figure 14 shows the variation of the surface roughness of ECM-machined 12% Cr stainless steel test parts with respect to the applied current density.

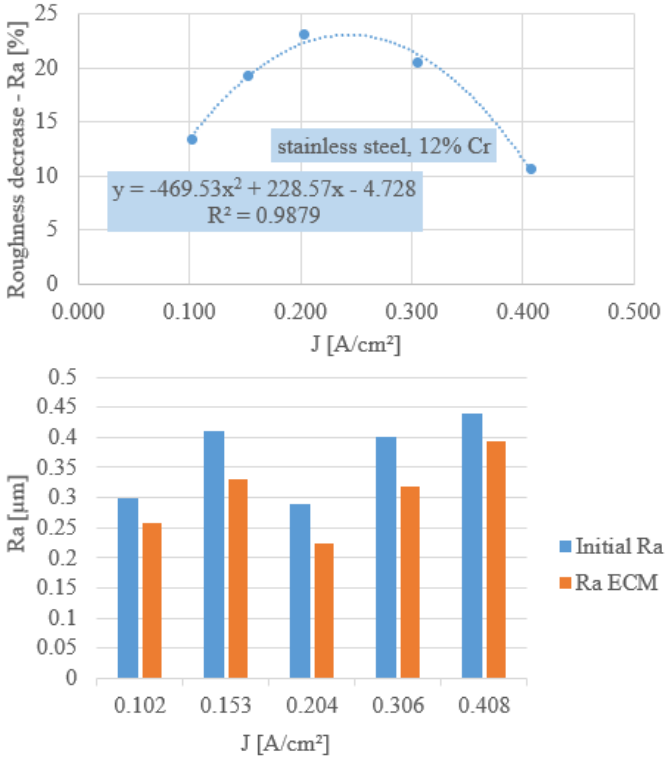

Figure 14. Influence of current density, J, on Ra, s_F = 0.6 mm, 5% NaCl solution, 12% Cr stainless steel

The Ra values show that there is a range of J = 0.153-0.306 A/cm² in which a percentage reduction in roughness of 19-23% is observed. Under the described machining conditions, an optimal value of current density can be established at J = 0.2 A/cm², with the objective function being the percentage reduction of Ra by 23% for the measured average values.

Hybrid machining

Test parts of 12% Cr stainless steel were processed by electrochemical machining combined successively with ultrasonic treatment, with the total machining time divided equally [9]: 1 minute and 30 seconds of electrochemical machining, followed by ultrasonic processing at PcUS = 87.6 W, reaching a total time of 3 minutes, as also indicated in table 3.

Table 3. ECM + successive US machining, PcUS = 87.6 W, 12% Cr stainless steel

Number of testing part	J [A/cm²]	I [A]	Time [min]	Initial Ra [µm]	Ra ECM+US [µm]	Decrease of Ra ECM+US [%]
1	0.102	0.5	3	0.61	0.57	6.557
2	0.204	1	3	0.642	0.57	11.215
3	0.306	1.5	3	0.508	0.438	13.780
4	0.408	2	3	0.398	0.36	9.548
5	0.510	2.5	3	0.514	0.482	6.226

Figure 15 shows the variation of current density in relation to the percentage reduction of roughness parameter, Ra, during successive electrochemical-ultrasonic machining of 12% Cr stainless steel.

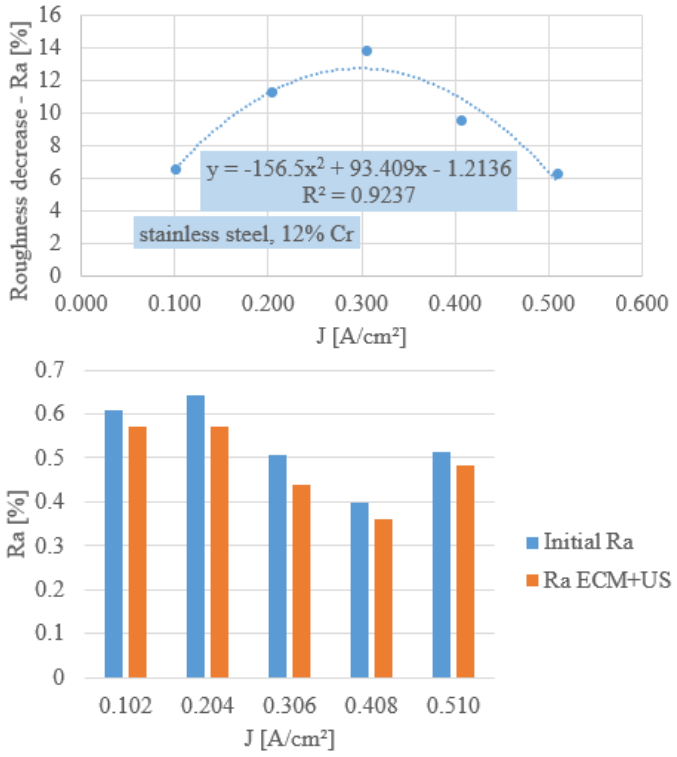

Figure 15. Influence of current density, J, on Ra, s_F = 0.3 mm, 5% NaCl solution, 12% Cr stainless steel

It can be observed that at a current density of J = 0.306 A/cm², a reduction in surface roughness of approximately 13% is achieved. The optimization of current density J was pursued, with the objective function being the percentage reduction of Ra roughness relative to its initial value. It was found that an ultrasonic power below 90 W does not allow a substantial reduction of Ra for surfaces processed by successive ECM+US finishing. Then, a new procedure for successive electrochemical-ultrasonic machining was established, carried out as follows [9]: supplying the ECM cell with 5% NaCl electrolyte; Pause for 30 seconds; Ultrasonic processing for 1 minute and 30 seconds; Electrolyte washing for 30 seconds; Pause for 30 seconds; Electrochemical machining for 1 minute and 30 seconds; Repeat the cycle three times.

- The influence of ultrasonic power consumption on the surface roughness in ECM+US finishing of 12% Cr stainless steel test parts.

The ultrasonic power was varied at a current density of J = 0.306 A/cm² for the electrochemical-ultrasonic finishing of 12% Cr stainless steel test parts, and the results obtained are presented in table 4.

Table 4. ECM + successive US machining, 12% Cr stainless steel

Number of testing part	PcUS [W]	J [A/cm²]	s_F [mm]	Initial Ra [µm]	Ra ECM+US [µm]	Decrease of Ra ECM+US [%]
1	94.8	0.306	0.7	0.432	0.4	7.407
2	103.2			0.237	0.2	15.612
3	109.2			0.215	0.16	25.581
4	114			0.437	0.31	29.062
5	118.8			0.494	0.37	25.101

Figure 16 presents a graphical representation of the results obtained from varying the ultrasonic power.

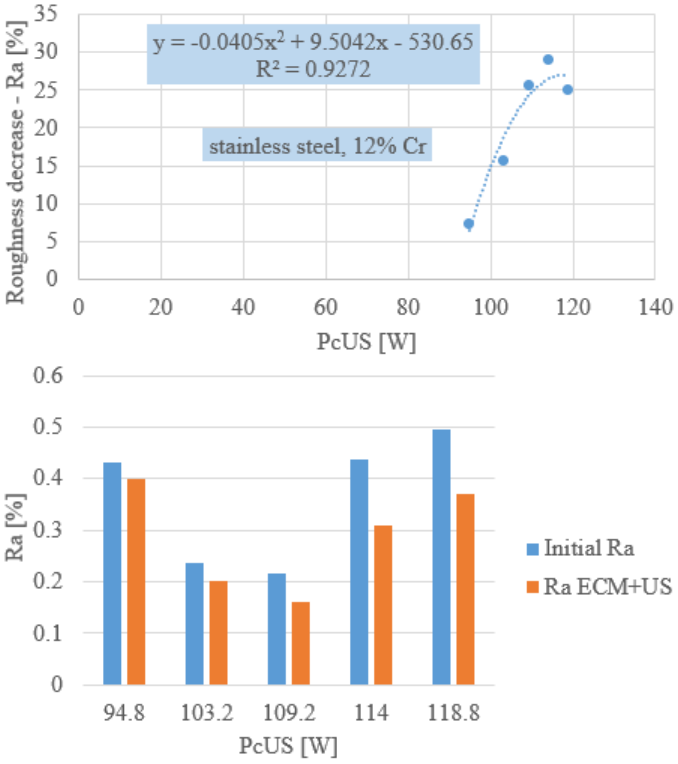

Figure 16. Influence of ultrasonic power, PcUS, on Ra, s_F = 0.7 mm, 5% NaCl solution, 12% Cr stainless steel

It can be observed that there are increases in the percentage reduction of surface roughness of approximately 25-29% within the range of PcUS = 109.2-118.8 W.

5. CONCLUSIONS

The nonconventional technologies, electrochemical or electrochemical-ultrasonic machining requires monitoring and control of the following parameters: current intensity, processing time, working gap, temperature, electrical resistivity, electrolyte concentration, ultrasonic generator frequency, and ensuring resonance frequency between the transducer and the concentrator. Constant replacement of the electrolyte, as well as ensuring its recirculation and filtration, can influence the surface quality of the test specimen. Additionally, the use of acid-based electrolytes can have positive effects on the roughness of the machined surfaces of the parts,

although they present the disadvantages of more difficult handling and higher costs.
The hybrid electrochemical-ultrasonic machining process contributes through both components to the reduction of surface roughness: anodic dissolution begins at the peaks of the microgeometry where the electric field is more intense (there is a critical time after which the achieved roughness increases); ultrasonic-induced cavitation in the machining gap preferentially removes the microgeometry peaks (there is an optimal value of power consumed by the ultrasonic chain, as higher powers result in increased roughness).

6. REFERENCES

[1]. Zhang, Y., *Investigation Into Current Efficiency For Pulse Electrochemical Machining Of Nickel Alloy*, Industrial and Management Systems Engineering, M.S. Thesis, University of Nebraska – Lincoln, (2010).

[2]. Insoon, Y., et. al., Micro ECM with Ultrasonic Vibrations Using a Semi-cylindrical Tool, *International Journal of Precision Engineering and Manufacturing*, Vol. 10, No. 2, p. 5-10, (2009).

[3]. Skoczypiec, S., Research on ultrasonically assisted electrochemical machining process, *The International Journal of Advanced Manufacturing Technology*, Vol. 52, p. 565-574, (2011).

[4]. Ghoshal, B., Bhattacharyya, B., Influence of vibration on micro-tool fabrication by electrochemical machining, *Elsevier*, *International Journal of Machine Tools and Manufacture*, Volume 64, p. 49-59, (2013).

[5]. Hassan, E.H., Vibration-assisted electrochemical machining: a review, *The International Journal of Advanced Manufacturing Technology*, Vol. 105, p. 579-593, (2019).

[6]. Saxena, K.K., Qian, J., Reynaerts, D., A review on process capabilities of electrochemical micromachining and its hybrid variants, *International Journal of Machine Tools and Manufacture*, Vol. 127, p. 28-56, (2018).

[7]. *** MatWeb, Your Source for Materials Information, Available at: https://www.matweb.com/search/DataSheet, accessed: 1.07.2024.

[8]. Drobota, V., *Strength of Materials*, Technical Publishing, (1982).

[9]. Enciu, C.C., *Research on hybrid electrochemical-ultrasonic finishing machining*, PhD Thesis, UNSTPB, (2024).